Mat Res Innovat (1999) 2:256–262

ORIGINAL ARTICLE

K.M.S. Khalil

Low temperature evolution of crystalline $BaTiO_3$ from alkali-metal free precursor using sol-gel process

Received: 21 July 1998 / Reviewed and accepted: 30 September 1998

Abstract Bulk structure and surface texture of $BaTiO_3$ materials synthesized at low temperature using sol-gel technique have been investigated. The materials were produced by the pyrolysis of an xerogel precursor of the tentative formula $BaTiO_{3-x}(CH_3COO)_{2x}$, which was prepared using 1:1 molar ratio of barium acetate and titanium oxyacetate solution. The present method avoids using alkali-metal hydroxides (as a hydrolyzing agent), and thus produces an alkali-metal free precursor. The decomposition course of the xerogel at the onset of formation of crystalline $BaTiO_3$ was probed applying thermogravimetry (TG), differential scanning calorimetery (DSC), Fourier-transform infrared spectroscopy (FTIR), and X-ray diffraction (XRD) techniques. Results indicated that most of the precursor weight loss occurs below 400°C, with the formation of titania rich intermediates. However, it was not until the temperature reached ≥600°C that well crystallized $BaTiO_3$ was produced. The specific surface area and porosity were assessed for $BaTiO_3$ produced at 600–1000°C using N_2 adsorption at liquid N_2 temperature.

Key words $BaTiO_3$ · Barium titanate · Titanium oxyacetate · Surface texture · Surface area · Porosity · Crystalline powder

Introduction

Barium titanate, $BaTiO_3$, is one of the most important materials in the electronic industry [1]. This is mainly due to its high dielectric constant and ferroelectric properties [2]. The most important application of $BaTiO_3$ material is as a multi-layer capacitor. Recently this application in dynamic random access memory (DRAM) has been further studied [1, 3]. However, thin films with both high dielectric constant and good insulating properties are required. The conventional technique for the preparation of $BaTiO_3$ by the solid-state reaction between $BaCO_3$ and TiO_2, which requires a temperature as high as 1400°C, seems to be inappropriate to the recent applications.

Thus non-conventional preparation methods involving milder heat processing are encouraged. Low temperature, wet chemical routes offer favorable alternatives for the synthesis of high purity, homogenous, ultrafine $BaTiO_3$ from which electronic components with tailored and predictable properties could be prepared [4]. Several of these methods are based on the use of alkoxides, acetates, citrates, oxalates, hydroxides and combinations, as parent materials were reported [5–13]. However, methods adopting barium acetate and titanyl acylate-type precursors are more promising, and offer several technological advantages. Barium acetate is a moisture insensitive and inexpensive precursor on one hand; and titanyl acylate dissolves readily thus avoiding the potential problem of hydrous titania, on the other [4].

The use of barium acetate and titanyl acylate precursors for the preparation of $BaTiO_3$ through a Sol-precipitation or a Sol-gel route was described [8–11]. Accordingly, the Sol-precipitation method is shown to involve the reaction of titanium isopropoxide with excess glacial acetic acid (Ac/Ti=10) to form a titanyl acylate (white precipitate under acidic conditions). The precipitate was dissolved in excess water and the barium acetate solution was added to obtain a stoichiometric sol. The sol was then hydrolyzed by the addition to a highly alkaline solution of sodium hydroxide to obtain stoichiometric $BaTiO_3$ powders.

The Sol-gel method involves the use of identical precursors [8–10], however with no alkali-metal addition. In acidic media, monolithic gels were formed. It has been reported [4], that gelation can be enhanced by increasing the temperature. Calcination of the dry gels resulted in crystallization and evolution of crystalline $BaTiO_3$.

Presented at the *Innovations in Materials Conference*, Washington, D.C., July 19–22, 1998

K.M.S. Khalil
Chemistry Department, Faculty of Science,
South Valley University, Sohag 82524, Egypt
Fax: 093-601-159, e-mail: younes@sohag.jwnet.eun.eg

The present investigation was designated to attempt utilizing a low acetic acid ratio (Ac/Ti=1) in isopropanol to partially replace the alkoxy groups by acetate groups. On addition of a stoichiometric amount of $Ba(CH_3COO)_2$ solution (water solution) a gel was formed. The dried xerogel was characterized and the evolution of crystalline $BaTiO_3$ from this precursor was investigated. Since no alkali-metal was added, the precursor is termed as being an alkali-metal-free precursor. The bulk crystallization structure of $BaTiO_3$ formed was characterized by XRD. The surface texture was assessed by analysis of N_2 adsorption data.

Experimental

Materials

The Xerogel precursor. 0.005 mole of acetic acid was add to 50 ml of isopropanol solution containing 0.020 mole of $Ti(OPr^i)_4$ (Aldrich, 99.99%). The solution was stirred at 400 rpm for 30 min at room temperature. Then, a 50-ml portion of an aqueous solution containing 0.020 mole of $Ba(CH_3COO)_2$ (Carlo Erba, 99%) was added to the above solution. A white gel was immediately formed. The gel temperature was raised to 60°C, and then allowed to stir for an additional 60 min. The resultant gel was pored into a glass dish, covered with a filter paper and the solvent was evaporated at room temperature. After three days a translucent dry gel was formed, which was ground and allowed to dry at 90°C overnight. This dry precursor is termed above, *"The xerogel precursor"*.

Portions of the xerogel were examined by Thermal analyses. The decomposition course was probed using infrared spectroscopy for the solid decomposition products. A set of products were prepared by ex-situ heating of the xerogel in N_2 atmosphere for 90 min at different temperatures (150–1000°C), and then cooled directly to room temperature.

Another set of xerogel calcination products were obtained at 200–1000°C for 2 h. Structures of these calcination products were examined by X-ray diffractometry. This set of materials is termed below as *The calcined materials*. The surface texture of the materials calcined at ≥600°C was examined by N_2 adsorption techniques. To study the sintering impacts on the material properties, a separate sample was calcined by gradual heating (at 5°C/min) up to 1000°C, and maintained for 2 h (at 5°C/min), prior to cooling to room temperature. The later material is denoted below *"The 1000° C sintered material"*, and its surface texture was assessed also using N_2 gas technique.

The Titanyl acylate precursor, $TiO(CH_3COO)_2$, was prepared using the same procedure applied for reacting acetic acid with $Ti(OPr^i)_4$, in a 1:1 ratio in isopropanol. The resulting sol was hydrolyzed by the addition of an equal volume of water. The gel obtained was dried utilizing the same procedure as described above. A portion of the titanyl acylate thus produced was used for comparative purposes. Complete characterization of the hydrolyzed decomposition products of a similar precursor was earlier reported [14].

Techniques

Thermal analyses. A Thermal Analyst 2000 TA instrument (USA) controlling a 2050 thermogravimetric (TG) analyzer and 2010 differential scanning calorimeter (DSC) was used. For TG a ceramic sample boat was used with the sample size being 10.0±0.1 mg. Curves were recorded upon heating up to 900°C at 5°C/min and 30 ml/min flow of nitrogen or oxygen atmosphere. Transition temperature analysis was carried out for each region in each TG curve, using the TGA 5.1 software of the instrument indicated. For DSC measurements, a sample size of 5.0±0.1 mg is heated up to 500°C in a covered aluminum sample pan at 5°C/min and a flow of 30 ml/min of nitrogen gas.

FTIR Spectroscopy. FTIR spectra were recorded in 4000–400 cm^{-1} against a pure KBr disc, using an instrument model Shimadzu-FTIR800 (Japan).

X-ray Powder diffractometry. XRD was carried out using a XRD diffractometer model D5000 Sieminse (Germany) with Ni-filtered CuK_α radiation (λ=1.5418 Å). An on-line data acquisition and handling system (Diffrac software, Siemens) and JCPDS-ICDD standard data [15], were used for phase identification purposes.

Nitrogen gas adsorption. N_2 gas adsorption/desorption isotherms were measured at –196°C using a model ASAP 2010 (Micromeritics Instrument Corporation, USA). Test samples were thoroughly outgassed for 2 h at 150°C. The specific surface area, S_{BET}, was calculated applying the BET equation [16]. Pore Volume distribution curves were generated by DFT plus V1.00 (2010) software of the instrument indicated, implementing the original density function theory, and slit pores shape [17].

Results and discussion

The xerogel pyrolysis and $BaTiO_3$ formation

The xerogel was found to be amorphous under XRD. Figure 1 shows the TG and DTG curves recorded for the xerogel precursor heated up to 900°C at 5°C/min and 30 ml/min flow of nitrogen (Fig. 1A) or oxygen atmosphere (Fig. 1B). TG and DTG curves recorded for the pure $Ba(CH_3COO)_2$ and the oxytitanylacetate compounds are shown in Fig. 2A and 2B, respectively. The TG curves indicate that the xerogel decomposes in four stages in each case. Table 1 shows the transition point analysis results along with the weight percentage at the stop point of each decomposition step in the TG curves. Depending on the FTIR and XRD results (see below) the final products were identified in each case as $BaTiO_3$. Thus tentative formulae of the intermediate products could be determined as shown in Table 1.

Figure 3 shows the DSC curve for the xerogel precursor heated up to 500°C in a covered pan at 5°C/min and a flow of 30 ml/min of nitrogen gas. An endothermic peak was observed on heating from room temperature till <200°C, with maxima at 101 and 147°C; these may be related to the evaporation of water and solvent molecules. Above 200°C (in the range of the 2nd TG step), three DSC peaks were observed; an endotherm at 332°C followed by two exotherms at 373 and 458°C. It can be seen that the conversion from gel to glass would be completed at <500°C.

Figure 4 shows FTIR spectra for the as prepared gel dried overnight at 90°C and 150°C (spectra a and b, respectively). FTIR spectra for the different samples which were heated isothermally in N_2 atmosphere for 90 min at 150–400°C were recorded. The spectrum of the materials obtained at 300°C is shown in Fig. 4 (spectrum c). Not much difference was observed in IR spectra of the materials obtained at 150–300 C. The main vibrations observed in spectra b and c of (Fig. 4) may be assigned to OH^- stretching at 3420 cm^{-1}, and acetate asymmetric

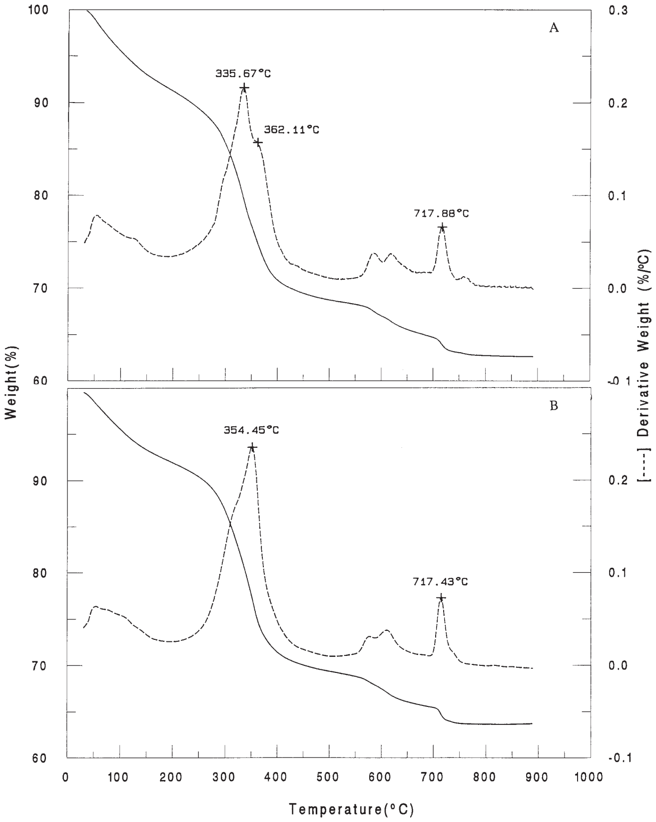

Fig. 1A, B TG and DTG curves recorded for the xerogel precursor on heating up to 900°C at 5°C/min and 30 ml/min flow of nitrogen (**A**) or oxygen (**B**) atmosphere

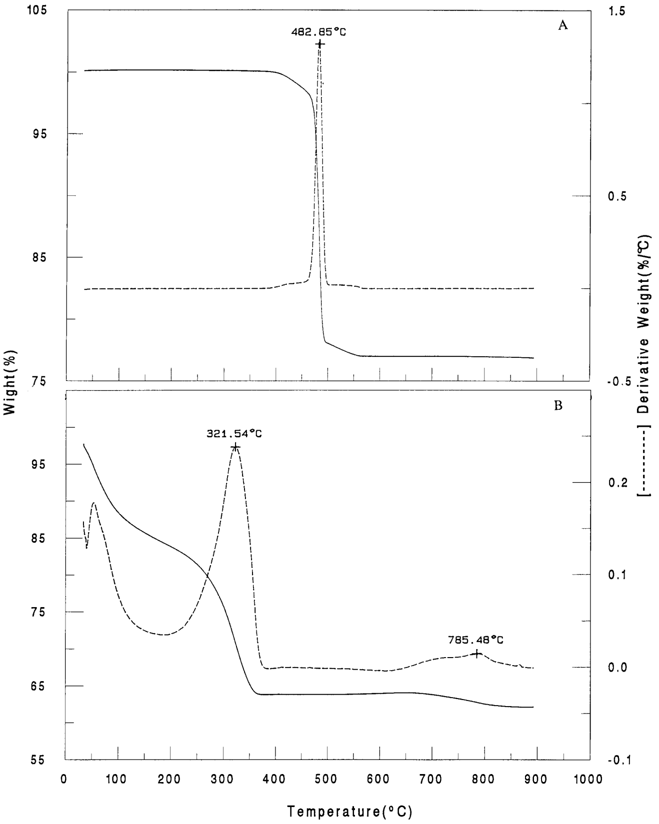

Fig. 2A, B TG and DTG curves recorded for the pure Ba(CH_3 COO)$_2$ (**A**), and the oxytitanylacetate compound (**B**) on heating up to 900°C and 5°C/min and 30 ml/min flow of nitrogen

Table 1 Transition point analysis for each start-stop range indicated, along with the weight percentage and tentative formula at the stop point of each range in the TG curve of the precursor material obtained at different atmosphere

Formula	W% (°C)	End (°C)	Mid-point (°C)	Onset (°C)	Start-Step (°C)	Step (°C)	Atmosphere
$BaTiO_{1.95}(CH_3COO)_{2.10}$	91.32	110	80	46	30–192	I	Nitrogen
$BaTiO_{2.52}(CO_3)_{0.48}$	68.47	380	339	298	192–523	II	
$BaTiO_{2.81}(CO_3)_{0.19}$	65.04	337	605	580	523–679	III	
$BaTiO_3$	62.78	729	721	711	679–800	IV	
$BaTiO_{1.97}(CH_3COO)_{2.06}$	91.96	122	85	45	30–196	I	Oxygen
$BaTiO_{2.53}(CO_3)_{0.47}$	69.36	381	342	305	196–506	II	
$BaTiO_{2.84}(CO_3)_{0.16}$	65.72	633	603	574	506–684	III	
$BaTiO_3$	63.75	727	720	711	684–800	IV	

and symmetric stretching modes at 1563 and 1416 cm^{-1}, respectively; C–H bending at 1028 cm^{-1}, and M–O stretching at 650 cm^{-1} [1, 18]. The same group of vibrations was observed in the spectrum of the 90°C dried precursor (Fig. 4 spectrum a) plus a set of minor vibrations which could be attributed to the stretching and bending vibrations of water and isopropyl solvents.

Figure 5 shows FTIR spectra obtained for the set of materials heated isothermally for 90 min in N_2 at 350–400°C. Many more differences are recognized with the increase of temperature in this range. The acetate vibrations at 1563 and 1416, observed for the 300°C heated material (Fig. 4), were gradually shifted to 1547 and 1424 cm^{-1} at 350°C. Then smeared and at higher temperatures, two new peaks are developed at 1431 and 858 cm^{-1} for the 375°C (and 400°C) heated material. The latter two peaks, observed for the 375°C heated material, can be related to the stretching ($v_{C=O}$), and out-of-plane deformation of $CO^{2-}{}_3$ groups, respectively [18].

Figure 6 shows spectra FTIR recorded for the materials heated isothermally at 600–1000°C; two bands at 538 cm^{-1} and ~400 cm^{-1} assignable to $BaTiO_3$ [18], developed at 600°C. Nevertheless, the vibrations related to CO_3^{2-} (at 1437 cm^{-1}) were still observed for the 600°C product, and can be recognized to a lesser extent, for the 800°C product. The spectra obtained for the 1000°C product indicates the formation of carbonate-free $BaTiO_3$.

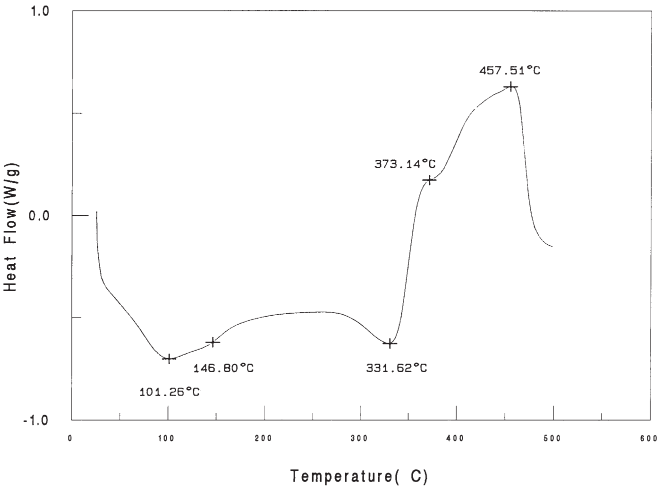

Fig. 3 DSC curve for the xerogel precursor obtained on heating up to 500°C and 5°C/min at the flow of 30 ml/min of nitrogen gas

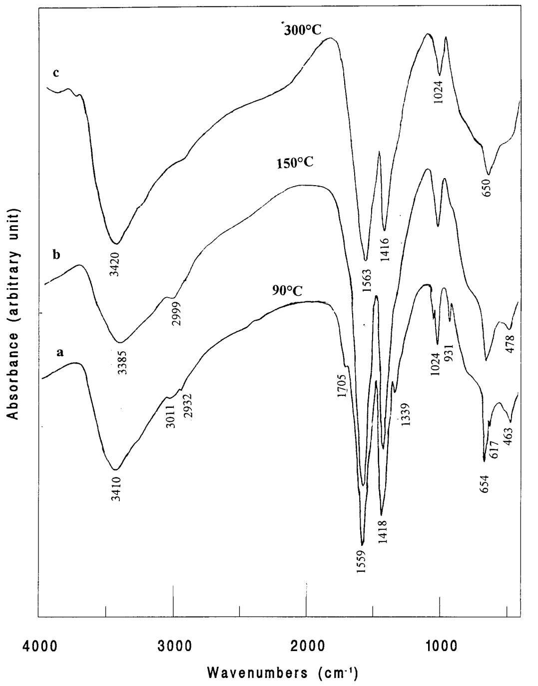

Fig. 4 FTIR spectra for the gel dried overnight at 90°C (*a*), 150°C (*b*), along with spectra for the samples heated in N_2 atmosphere isothermally (for 90 min) at 300°C

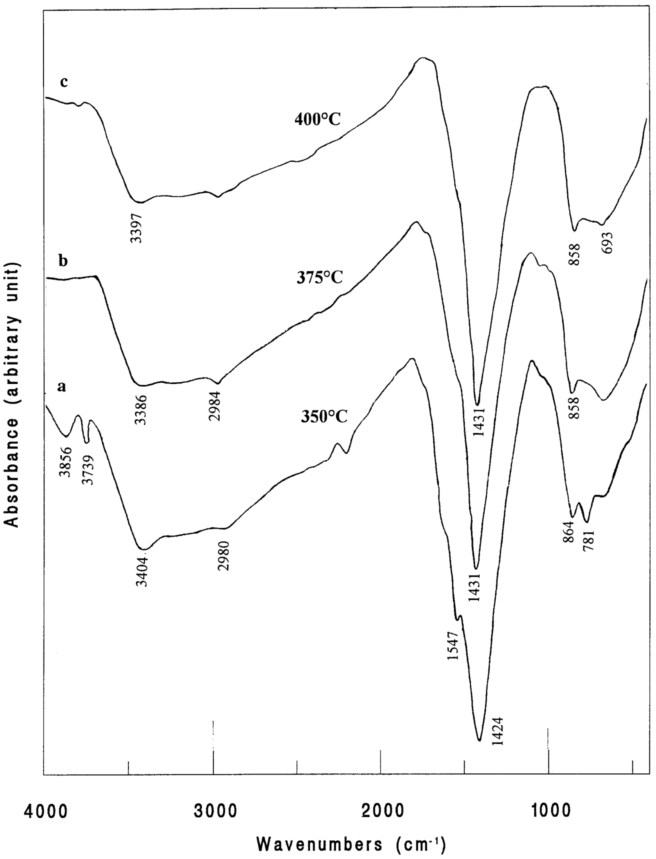

Fig. 5 Spectra obtained for the set of materials heated isothermally for 90 min in N_2 atmosphere at 350°C (*a*), 375°C (*b*), and 400°C (*c*)

Structure and texture assessment of the calcination products

Figure 7 shows XRD diffractograms for the materials calcined at 200–1000°C for 2 h in a static air atmosphere. The pattern for the material calcined at 200°C reveals an amorphous nature. The XRD pattern for the material calcined at 400°C shows peaks related to $BaCO_3$; however few other peaks were observed which could be assigned to titania-rich phase ($BaTi_5O_{11}$ card 35–0805). Thus, the pattern for the materials calcined at 600°C shows most of the peaks charactersic for $BaTiO_3$. However, peaks characteristic for $BaCO_3$ with low relative intensity are still observable. XRD patterns for the materials calcined at 800 and 1000°C show peaks revealing good, crystalline, tetragonal, $BaTiO_3$ (Card No., 05–0626).

Figure 8 shows nitrogen adsorption/desorption isotherms for the 2 h calcination products at 600 and 800°C, along with the 1000°C sintered material. The isotherm for the 600°C calcination product is of type IV of isotherm [19–21]. However, the unrestricted adsorbed volume over the p/p^o range, similar to type II, may indicate the presence of macro-porosity. Moreover, the isotherm shows H3 hysteresis loop, observed with aggregates of plate-like particles giving rise to slit-shaped pores [19].

The isotherm for the 800°C calcination product is rather similar to the previous isotherm; nevertheless, the adsorption capacity and the width of the loop are reduced. It should be noted that the range on which the isotherm is concave to the p/p^o axis is wider for the 800°C calcination product. This trend may be recognized much more clearly for the 1000°C sintered material. This behavior is similar to type I of isotherms, associated with the presence of micro-porosity. The unrestricted uptake at the p/p^o range is still observed for the isotherms of the

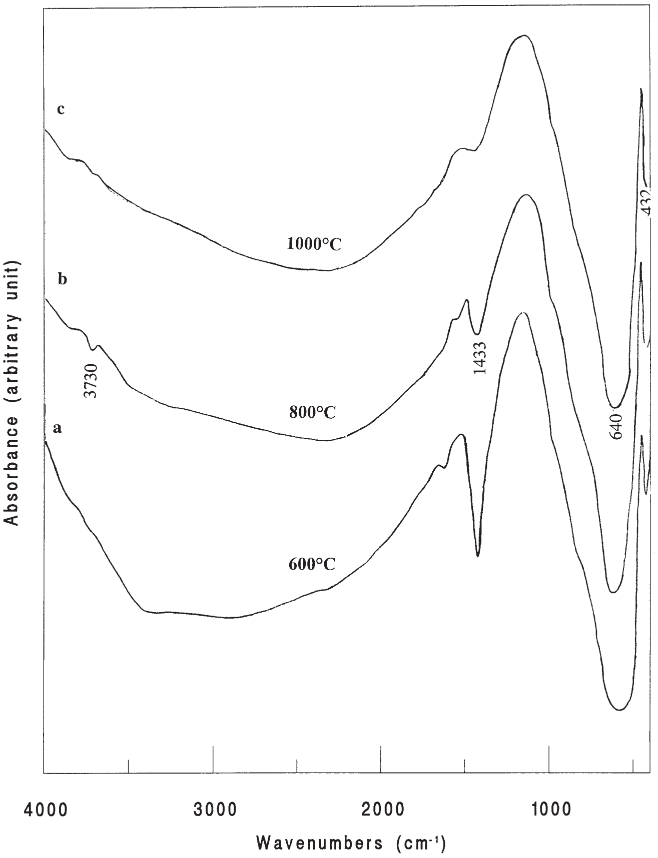

Fig. 6 Spectra recorded for the materials heated isothermally for 90 min in N_2 atmosphere at 600°C (*a*), 800°C (*b*), and 1000°C (*c*)

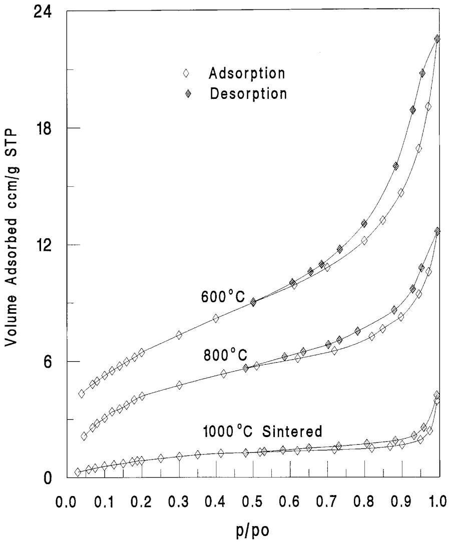

Fig. 8 N_2 adsorption/desorption isotherms for the 2 h calcination products at 600°C and 800°C, along with the 1000°C sintered material

Table 2 Surface area, S_{BET}, and c_{BET} constant, for the different calcination products

Calcination	S_{BET}	c_{BET}
600 °C / 2 h	23.95	56.54
800 °C / 2 h	17.28	20.67
1000 °C / 2 h	14.61	11.40
1000 °C Sintered	4.04	11.29

800°C calcined and 1000°C sintered material. Thus the latter two material isotherms show a complex type of isotherm indicating the presence of micro-, meso- and macro-pores.

Table 2 shows the surface area, S_{BET}, and the c_{BET} constant values for the calcined materials. The S_{BET} is shown to decrease from 23.9 to 14.6 m^2/g on increasing of the calcination temperature from 600 to 1000°C. However, an S_{BET} of 4.0 m^2/g was determined for the 1000°C sintered material.

Figure 9 shows differential pore volume (DPV) distribution (in cm^3/g) versus pore width (in nm) for the materials calcined at 600°C and 800°C, as well as the material sintered at 1000°C. On increasing the calcination tem-

Fig. 7 XRD diffractograms for the group of materials calcined for 2 h at 200–1000°C in a static atmosphere of air

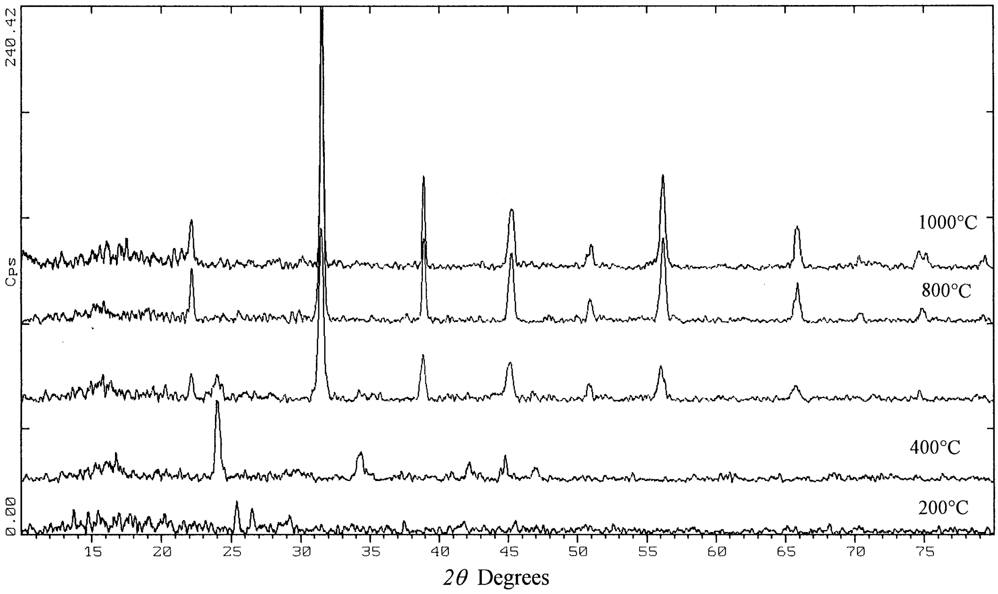

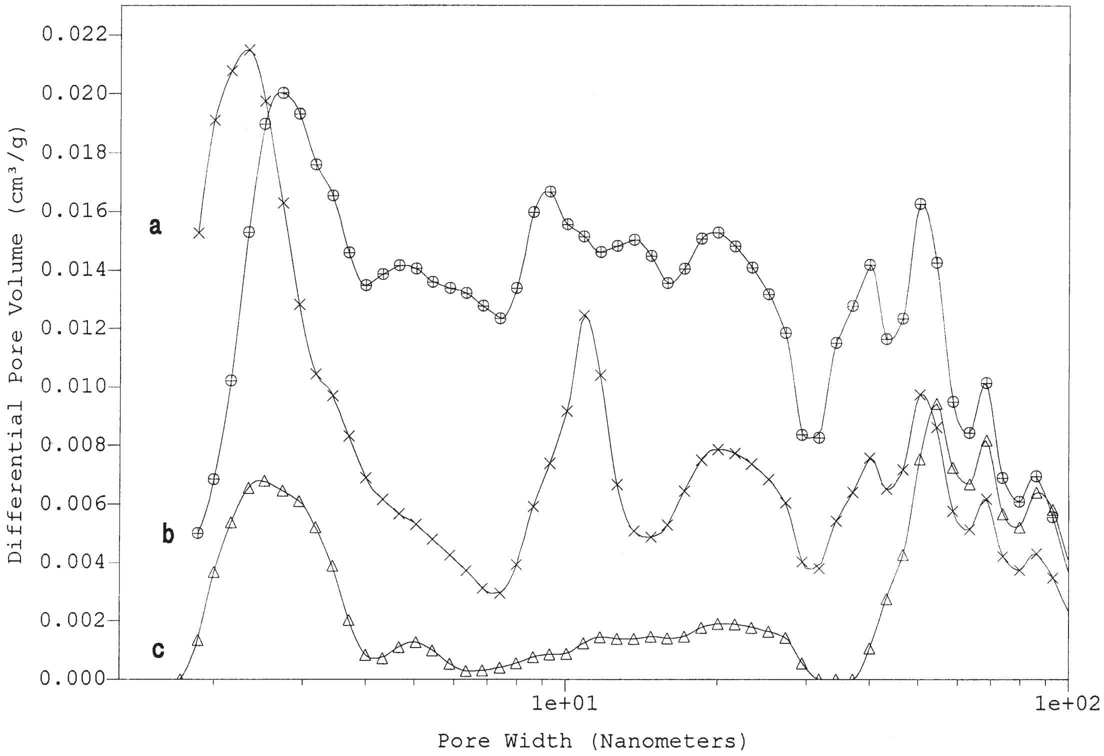

Fig. 9 Differential pore volume (DPV) distribution in cm^3/g versus pore width in nm for the materials calcined at 600°C (*b*), 800°C (*a*), along with the 1000°C sintered material (*c*)

perature from 600°C to 800°C, the DPV curves reflect the creation of more micro-porosity as the distribution shifts towards the micro-pore limit [21], reduction in the number of peaks the meso-pore range (2–50 nm), and a small change for the distribution peaks on the macro-pore range (>50 nm). Referring to the DPV for the 1000°C sintered material, one can realize that the micro-porosity was reduced; a smooth distribution through the meso-porous range was obtained, and slight change for the distribution peaks in the macro-pore range. These results, along with the S_{BET} results, reflect the progressive sintering of the materials upon increasing the temperature and duration of calcination; the surface area is being largely reduced.

Conclusions

1. Synthesis of pure barium titanate was successfully achieved from the xerogel formed by the addition of barium acetate solution to a titanyl acylate sol (prepared with 1:1 acid modified Ti(IV) isopropoxide). The dry xerogel precursor was, tentatively, found to be $BaTiO_2(CH_3COO)_2$. It was found that the pyrolysis sequence of this barium-titanium-oxyacetate-type precursor goes (in N_2 atmosphere) through the following stages:

Stage 1 (30–192°C)
The Xerogel Precursor $\longrightarrow BaTiO_{1.95}(CH_3COO)_{2.10}$

Stage II (192–523°C)
$BaTiO_{1.95}(CH_3COO)_{2.10} \longrightarrow BaTiO_{2.52}(CO_3)_{0.48}$
or $1/2BaTi_2O_5+1/2BaCO_3$

Stage III (523–679°C)
$BaTiO_{2.52}(CO_3)_{0.48} \longrightarrow BaTiO_{2.81}(CO_3)_{0.19}$

Stage IV (679–800°C)
$BaTiO_{2.81}(CO_3)_{0.19} \longrightarrow BaTiO_3$

A similar decomposition sequence was observed in oxygen atmosphere, with some enhancement in stages II and III.

2. It should be noted that no titania phases (anatase or rutile) were observed at any stage (see XRD results). This indicates that no phase separation was present or occurs through the decomposition process, which led eventually to formation of $BaTiO_3$.

3. Calcination of the xerogel at a low temperature (as low as 600°C) produced crystalline $BaTiO_3$ (containing some $BaCO_3$). Calcination at higher temperatures produce pure $BaTiO_3$. XRD measurements at room temperature indicated that tetragonal $BaTiO_3$ was the sole phase present.

4. Surface texture of the calcined materials is a function of temperature and calcination procedure. Thus a 2 h calcination at 600°C produced porous materials of surface area of 23.9 m^2/g. On increasing the calcination temperature up to 1000°C, the surface area and porosity gradually decreased to S_{BET}=14.6 m^2/g. Some increase in micro-porosity was recognized for the material calcined at 800°C in comparison to that calcined at 600°C (due to the decomposition of residual carbonate above 600°C).

However, micro-porosity decreased for the 1000°C sintered material due to sintering. Thus, the latter material showed strong sintering effects; consequently, the surface area and porosity were largely reduced (c.f., S_{BET}=4.0 m^2/g).

Acknowledgements The author would like to express thanks to Prof. M.I. Zaki at Kuwait University (Kuwait) and Prof. A.A. El-Samahy at South Valley University (Egypt) for their fruitful discussions and support.

References

1. Takeuchi T, Tabuchi M, Ado K, Honjo K, Nakamura, Kageyama H, Suyama Y, Ohtori N, Nagasawa M (1997) J Mater Sci 32: 4053
2. Nowotny J, Rekas M (1992) Key Engng Mater 66/67: 45
3. Bacsa R, Ravindranathan P, Dougherty JP (1992) J Mater Res 7: 423
4. Phule PP, Risbud SH (1990) J Mater Sci 25:1169
5. Shimooka H, Kuwabara M (1996) J Am Ceram Soc 79: 2983
6. Kim S, Lee M, Noh T, Lee C (1996) J Mater Sci 31: 3643
7. Shimooka H, Kuwabara M (1995) J Am Ceram Soc 78: 2849
8. Phule PP, Risbud SH (1988) Adv Ceram Mater 3: 183
9. Phule PP, Risbud SH (1989) Mater Sci Engg B3: 241
10. Phule PP, Risbud SH (1988) Material Research Socity. In: Brinker CJ, Clark DR, Ulrich DR (ed) Better Ceramics Through Chemistry, vol. 3 Pittsburgh, pp 275
11. Mosset A, Luneau IG, Galy J (1987) J Non-Cryst. Solids 89: 206
12. Viswanath RN, Ramasamy S (1997) Nanostruct Mater 8: 155
13. Nishizawa H, Katsube M (1997) Solid State Chem 131: 43
14. Khalil KMS, Baird T, Zaki MI, EL-Samahy A, Awad A (1998) Colloid and Surf A 132: 31
15. JCPDS, International Center for Diffraction Data, CD, 1996
16. Brunauer B, Emmett PH, Teller E (1938) J Am Chem Soc 60: 309
17. Refer to: Micromertics DFT Plus, Operator’s Manual (1996) V1.00
18. Nyquist RA, Kagel RO (1971) Infrared Spectra of Inorganic Compounds. Academic Press, Newyourk, London
19. IUPAC (1985) Pure Appl Chem 57: 603
20. Sing KSW (1980) In: Thomas JM, Lambert RM (eds) Characterization of catalysts. Wiley, pp 12
21. Lecloux AJ (1981) In: Androson JR, Boudart M (eds) Catalysis-Science and Technology. Springer, Berlin, Heidelberg, New York, pp171